Augmented Reality Application for Aiding Tumor Resection in Skull-Base Surgery

Niveditha Kalavakonda
Dept. of Electrical and Computer Engineering
University of Washington
Seattle, WA - USA
nkalavak@uw.edu

Laligam Sekhar
Dept. of Neurosurgery
Harborview Medical Center
Seattle, WA - USA
lsekhar@u.washington.edu

Blake Hannaford
Dept. of Electrical and Computer Engineering
University of Washington
Seattle, WA - USA
blake@uw.edu

Abstract—Treatment of cancer patients has improved with advances in tumor resection techniques for skull-base surgery. However, a secondary procedure or chemotherapy is often required to treat residual tumor to prevent recurrence. With the advent of assistive technology, such as augmented reality, a myriad of possibilities have been facilitated for the field of surgery. This work explores the development of an augmented reality application to improving the tumor margin excised during surgical procedures, with a focus on skull-base surgery. An isosurface reconstruction algorithm was integrated with the Microsoft HoloLens, a self-contained holographic computer, to enable visualization of Computed Tomography (CT) imaging superimposed in 3D on the patient. The results suggest that though the device has limitations at its current stage, the Microsoft HoloLens could be used for planning and overlaying the imaging information on the patient for removal of lesions in real-time. The modules developed could also be extended to other types of surgery involving visualization of Digital Imaging and Communication in Medicine (DICOM) files.

Index Terms—augmented reality, DICOM, mesh simplification, marching cubes, tumor resection

I. Introduction

Minimally Invasive Surgery (MIS) has revolutionized the way surgery is conducted. MIS has led to reduced visible scars on a patient, shorter stay at the hospital, improved recovery period after surgery and reduced trauma. It has conferred considerable advantages on the patient [1] [2] but has also imposed additional difficulty for surgeons operating in a limited workspace [3]. However, with the continual advancement of chip manufacturing, instrumentation, robotics and computer vision, there has been improved preoperative planning possibilities which enhance the skills of a surgeon and ameliorate complex procedures.

Image-guided surgery (IGS) has evolved steadily with advancing technology to augment a surgeons ability for dexterously administering surgical procedures. It assists with decreasing the invasiveness of surgical procedures, and improves safety and accuracy [4]. IGS tends to produce accurate results but it can be tedious for surgeons to accurately perceive depth and avoid critical structures compared to open surgery [5]. Since the view of 3D organs is projected on a 2D screen, there is information loss regarding the precise location of the tumor and critical structures. The visual displays of commercial navigation systems are generally situated away from the surgical field, compounding the problem. This presents surgeons with a difficult task of mismatched hand-eye coordination, thereby disrupting the surgical workflow [6].

Patients are subjected to repeat surgeries due to the possibility of residual tumors. A significant percentage of the population (up to 71.6% for hepatocellular carcinoma and about 50% for intracranial meningioma) [7] [8] are at risk after initial treatment for cancers affecting local regions. This increases cost further since locating the tumor and limiting its effects would be harder in the case of recurrences. An ideal solution is to minimize the risk of relapse and maximize conservation of healthy tissue.

Augmented/Mixed reality is an emerging field of study for surgical applications. Augmented reality allows the user to overlay virtual objects in a real-world environment, and mixed reality enables the user to anchor these rendered objects to the physical environment. Previous research suggests the potential benefits of using augmented or mixed reality devices to improve the precision of tumor margin excision [9]. However, the technologies developed were either too bulky, interfered with sterilization, lacked depth perception or had another significant limitation which restricted their use in the operating theater.

A. Contributions

To the best of the authors' knowledge, this work is the first to integrate a native implementation of an isosurface visualization algorithm with mesh simplification on the Microsoft HoloLens device to test image registration for tumor resection. This work incorporates additional functionalities such as 2D imaging data visualization, image registration, data anonymization and multi-user viewing.

II. RELATED WORK

The Augmented Reality system presented in [10] performs extensive studies on the use of a live video camera feed to provide additional information about a patients tumor for breast cancer surgery. The study analyzes the effects of tissue deformation that occurs between volume reconstruction from preoperative ultrasound scans and its use during surgery. The system required calibration between devices, similar to [11]. Reconstruction of the tumor is done by manual segmentation of images and is overlaid on the video feed. Though the tests in the phantom lab generated only a 2mm error, the clinical experiments proved that the system was not viable for real-time use. The patient was required to suspend breathing during the ultrasonic imaging to obtain scans with reduced error. This, however, resulted in errors during real-time use due to the inconsistent transformation matrices generated.

The prototype built by Fuchs et. al [12] shows the benefits of using a Head Mounted Display device for providing guidance to surgeons in the case of minimally invasive laparoscopic surgery. The device aimed to provide surgeons with a natural point of view, as presented during open surgery, by using a camera to create a virtual laparoscope by combining information from a conventional laparoscope and a projector emitting structured light (vertical stripes). Due to faulty depth extraction, imperfect depth calibration, and the delays in image display, the system was not suitable for use during surgery.

Elmi-Terander et. al [13] developed an Augmented Reality Surgical Navigation (ARSN) system which integrates an intraoperative imaging system and optical tracking for thoracic pedicle screw placement using augmented reality. A study on cadavers using ARSN showed a 33% improvement in accuracy for matched complexity level. Another group from INRIA [20] also looked into using 3D/2D registration for hepatic surgery guidance. However, both groups still relayed information to the surgeon on a conventional display device.

In [14], Wen et. al, use a projection-camera system to track patient anatomy for registration of preoperative data for Radio-frequency ablation procedures to remove liver tumors. Once registered, the anatomy, however, could not be manipulated or interacted with directly. Change in positioning anatomy would require manipulating the software, which is tedious for a surgeon. But the results of static experiments verify the increase in accuracy of procedures while using augmented reality.

A mixed-reality headset, developed for visualization of anatomy during laparoscopic surgery, is described in [15]. This work is the closest-related prior work that uses hardware similar to the Microsoft HoloLens and has a native algorithm to reconstruct virtual surfaces for augmentation. However, their system had problems with respect to presenting reconstructed volumes because of computations taking as long as 30 minutes. This system adds to the operating room cost. It does not produce interactive volumes, limiting the amount of information that can be communicated during surgery.
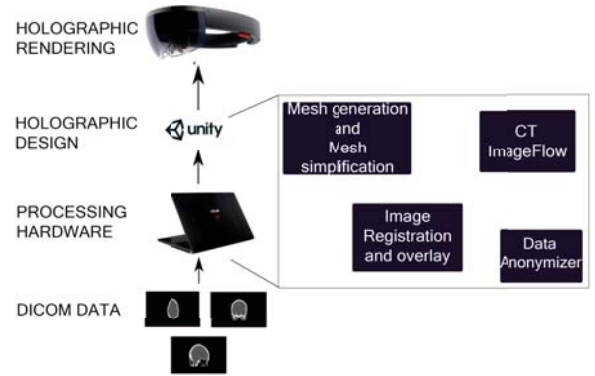

Fig. 1. Architecture diagram of system developed

III. METHODS

We developed software to input DICOM CT images and output live 3D overlays to the HoloLens device, used by a surgeon. A simplified architecture diagram is depicted in Fig.1.

The Unity3D Game Engine is the recommended platform for developing applications on the HoloLens. For our application, Unity3D was run on a laptop with 64-bit Windows 10 Student Edition, 16 GB RAM, Intel Core i7-4720HQ CPU 2.6 GHz Processor, and a NVIDIA GeForce GTX 960M graphics card. Windows Presentation foundation was used to verify the rendering algorithm and mesh simplification modules before being adopted into Unity3D. The entire application was developed in C#. A User Interface(UI) element allows users to choose DICOM images by filename from a secure drive on the cloud.

The DICOM images are converted to a mesh using a sequential-traversal method called Marching Cubes [16]. An isosurface is a surface of constant value, α that satisfies a scalar field $F(x, y, z) = f$, where F is a function of space (R^3) and f is a constant. Marching Cubes (MC) is an isosurface visualization algorithm that converts two-dimensional images into 3D volume by generating a mesh with triangles of constant density. It constructs the isosurfaces (decomposed into triangles) for a given F by sampling over a regular grid.

The meshes generated by Marching Cubes produce a large number of vertex points for most of our datasets. The resulting large number of polygons reduces performance when used on a standalone device such as the HoloLens, which has low on-board processing capability. To ensure performance in real-time, it is essential to reduce the number of triangles rendered in each frame. The mesh is simplified using mesh reduction techniques described in the section below.

A. Mesh Simplification

The mesh generated from marching cubes is simplified by *skinning* mesh components. This allows a mesh to be deformed based on an underlying transformation matrix set. We reduce the mesh size by evaluating and modifying the properties of
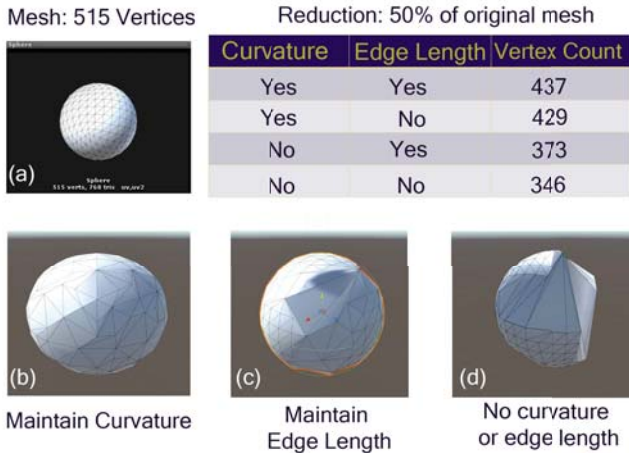
Fig. 2. Mesh simplification on sphere: (a) Sphere with 515 vertices, (b) 50% simplification with curvature, no edge length elimination, (c) 50% simplification with edge length elimination, no curvature, (d) 50% simplification with edge length elimination and no curvature.

the triangles. The parameters used for mesh reduction are edge length and curvature of the surface. Through the UI, the surgeon can choose the level of mesh reduction as a percentage of the original vertex count.

The simplification of the mesh is first processed by identifying and ensuring there are no repeated values for vertices. An internal dataset is constructed for ensuring the vertex data are truly different by identifying the UV values and color in addition to spatial locations. The entire process is developed by making the functions serializable in Unity3D. A class called *UniqueVertex* handles the processing of vertex points of the mesh. By generating new faces and vertices, the repetition of vertex points in the 3D space is overcome. The bone weights (also known as vertex weights) of all the vertex points contribute to obtaining information for mesh simplification.

The program recursively moves through each mesh in each tree (for the isosurfaces) to reduce all the child nodes equally. The mesh parameters used are curvature and edge length. Curvature determines the angles between the triangles and eliminates nodes in cases which produce a smoother transition between surfaces. Meshes in each surface plane can be combined to produce one large triangle instead. The edge length parameter eliminates a percentage of the small edges that form triangles to be combined with rather larger edges instead. A cost function from [17] is used for ensuring a maximum number of short edges are eliminated without affecting the surface rendered. For consolidating the mesh after simplification, the new vertex values are obtained and modified in the mesh based on their existence in the previous list. If the value is not available, a new index is created and the triangles are generated based on the relation of new vertex points.

For analysis, mesh simplification was tested on a simple sphere with 515 vertex points and 768 triangles. The results are shown Fig.2 on a simple sphere.The complete sphere is
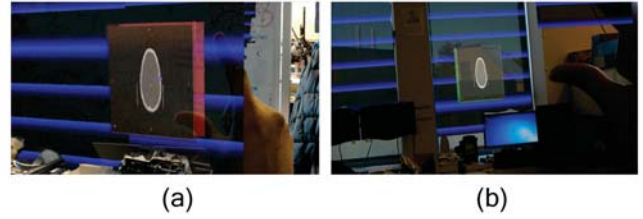

Fig. 3. CT Image Canvas (a) Non-placeable surface (b) Placeable surface

given in (a). With a 50% reduction in vertex points as target, deformations under the combination of parameter choices can be observed in images (b), (c) and (d). (b) denotes a case where curvature of the surface is maintained, without using the edge length parameter. (c) shows the result of thresholding edge length while not retaining curvature. (d) is a result of not using either the edge length or curvature parameters to retain the geometry. The algorithm ensures the surface stays intact and does not result in any holes/disconnected geometry as a result of mesh reduction. This is the prime reason for the reduction of vertex count to be different from the exact number obtained mathematically. For example, 50% reduction a default sphere from Unity3D (with 515 vertex points) results in more than 258 vertex points, as shown in the table for Fig. 2.

B. Application Workflow

The 3D mesh generated using the mesh reduction process is registered to fiducial markers located on the patient table. The volume is overlaid on a mannequin to depict performance of fiducials and the generated volume with respect to a patient. The results from our testing with the HoloLens is shown in section IV.

The application also includes a module to view all the slices from a patient's scan directly on the HoloLens device. Surgeons review CT slices intermittently during surgery in addition to the isosurface rendering provided since it augments a surgeons ability to confirm their findings from a 3D model. The 2D DICOM image viewer is defined as CT ImageFlow in Fig.1. A canvas game object in Unity3D acts as an interface element for dynamic viewing of scans. A red shadow is generated when the image cannot be placed on a wall surface and a green shadow denotes favorable locations for placement. The validity of positions is determined by computing the surface normal of desired target from the spatial map of the room provided by the HoloLens. It is determined to be favorable if the view is not distorted. The results of the *Placeable* function are shown in Fig. 3.

Additionally, to protect the privacy of the individuals during research and development of the system, a data anonymizer was developed to ascertain that information from the DICOM files cannot be traced back to an individual. Since the HoloLens is a self-contained device and is constantly
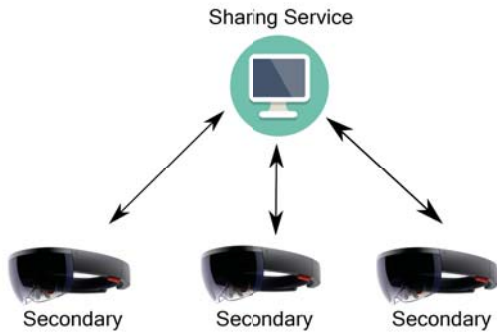
Fig. 4. Server-Client module is setup on the HoloLens to enable sharing of rendered objects.

Fig. 5. Marching Cubes rendered for bones using the Windows Presentation Foundation on a set of DICOM images. It consists of 1,916,374 triangles.

connected to the WiFi network, it is important to ensure re-identification of patient information through external attacks is not possible.

C. Collaborative Surgery

The Microsft HoloToolkit offers a library named *Sharing* for setting up communication between multiple HoloLens devices. The *Sharing Service* executable runs on a device that acts as the server for the entire communication process. A client library is included in applications running simultaneously on multiple devices. Communication between the server and client modules is established using sockets. Fig. 4 provides an overview of the server-client implementation.

A primary device starts the application and renders the virtual object representing the isosurface. This is placed at the desired location using gestures. The holograms could also be anchored using registration through fiducial markers. The world space coordinates of virtual object are then uploaded onto the server. Any secondary device connecting to the shared experience can download and view this isosurface from a different perspective. This would allow users to visualize the same isosurface in 3D to communicate and plan for surgeries better than they could otherwise. The functionality was tested with two different HoloLens devices.

IV. RESULTS

Patient data with 512 x 512 x 64 DICOM slices were used for evaluation of the algorithm. The marching cubes algorithm generated an isosurface to represent the desired anatomy of our patient. Fig. 5 represents an isosurface with an isovalue, α value of 500 Hounsfield units to represent bone.

A tumor consists of a different isovalue from healthy tissue. This would allow the tumor to be segmented in the exact location relative to bone as obtained from the imaging data and be included in the visualization. The number of vertices and triangles generated for both the isosurfaces are over a million points. This generated mesh was then reduced using mesh curvature and edge length simplification techniques as described in section III-A.
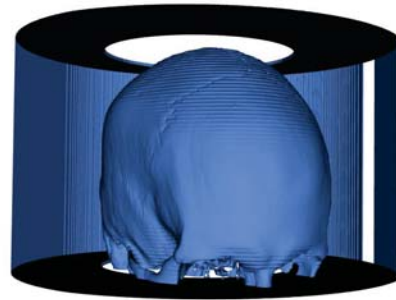
TABLE I
50% REDUCTION OF BONE ISOSURFACE
(1,437,115 VERTEX POINTS)

Curvature	Edge Length	Vertex Count
Yes	Yes	689,343
Yes	No	689,337
No	Yes	689,342
No	No	689,149

Though the vertex count for the combination of edge length and curvature parameters considered is different only by a small margin, the representation of the surfaces can be starkly different as shown in Fig.2 for the spheres. It is important to retain the exact structure of the volume despite modifying curvature or edge length thresholds. By breaking the 3D volume into smaller mesh components, it would be possible to reduce the size of the mesh only in select regions. The surgeon decides the Level of Detail desired for viewing while retaining anatomical integrity. By decreasing the amount of penalty imposed on removing a percentage of edges with shorter length, it would be possible to further reduce the number of triangles generated. However, this would also mean the surface generated may not provide refined information as is currently obtained when the curvature and edge length parameters are used. Downsampling the image datasets would reduce the number of pixels available for generation of meshes, thereby resulting in lesser number of triangles when using the Marching Cubes algorithm.

The HoloLens incorporates a feature called Spatial Mapping which provides a detailed representation of the environment in the format of a mesh. To reduce the rendering cost, the spatial map of the environment is mapped, stored and loaded for processing since the operating room environment does not change drastically between procedures. The placement of a patient with respect to the fiducial marker is known. This information combined with the transformation between the fiducial and the camera on a HoloLens provides the correct
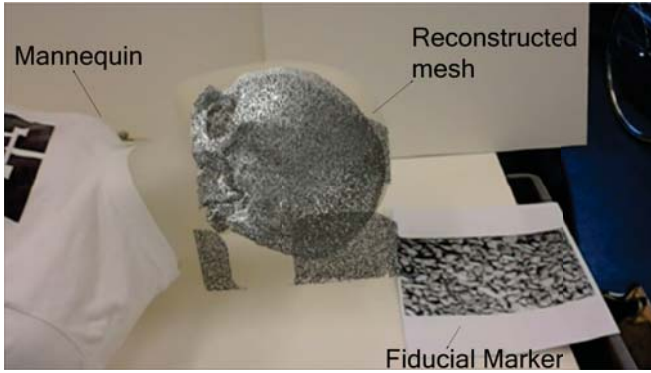
Fig. 6. Image overlay using fiducial markers. The fit is not exact since the shape of patient skull is different from the mannequin.

mapping between the HoloLens and patient. The resulting overlay of a patient data with the mannequin is shown in Fig.6. Unlike the case shown in the image, the overlay would be more exact in the case of matching reconstructions with the correct patient. Currently, the system has a delay of approximately one second when the user shifts view to an entirely different cross-section of the 3D object. This could also be a result of the large mesh size in combination with the additional functionalities incorporated.

V. DISCUSSION

The paper conceptualized the use a mixed reality headset with limited on-board processing for assisting surgeons for tumor resection. The results obtained through mesh rendering show the *Level of Detail* a generated mesh could possess about the anatomy of a patient. The 3D volume reconstructed from the CT scans relay fine details about the cracks, folds, and any tissue deformation present in the anatomy reliably. This can be visualized using the HoloLens device for either preoperatively planning surgeries or using the 3D model intraoperatively to gain enhanced information about the location of critical structures. However, slow performance on the HoloLens device evidenced the need for reduction of the size of meshes rendered. This is a result of the HoloLens being a mobile device with limited onboard processing capabilities. With mesh simplification techniques, the number of vertex points required for defining a structure is reduced for smooth rendering.

The process of combining meshes using a tagging process reduces the number of draw calls required for visualizing the surface information. By the process of manipulating the spatial mapping mesh, it is possible to overlay the isosurface generated on the target object, here, a mannequin. The surgeon can generate meshes to a certain degree of simplicity based on the level of detail desired in the final mesh rendered. By using the technique used in [17] the surgeon can specify the sections of the mesh that need to have a higher level of detail as opposed to a different section of the same mesh which could contain less refined information.

The application provides surgeons the ability to view the rendered surfaces and interact with the models by incorporating a range of techniques that have not previously been introduced onto the HoloLens device. This work is the first in the literature, to the best of our knowledge, to incorporate an array of functions that will be beneficial for the surgeon, including visualization and interaction with isosurfaces, registration to patient anatomy and on-board CT image viewer. Since the test methods were developed for smooth rendering of 3D models, it is not restricted to any one type of surgery. This allows us to extend the use of our current application to any type of surgery that could benefit from receiving augmented information. The information obtained from the datasets are also made Health Insurance Portability and Accountability Act (HIPAA) compliant and do not violate any standards set to protect patient privacy.

VI. FUTURE DIRECTIONS

Our algorithm to reduce mesh size of isosurfaces illustrates the advantages of generating a low polygon count while rendering objects. However, the size of the generated mesh can still be large for mobile devices to handle. Additional algorithms for improving the mesh performance can be implemented for a smoother interaction during real-time. The Delaunay triangulation [18] method restricts the number of points by avoiding points inside the circumcircle of triangles and can be explored to verify effect on mesh simplification. Other methods for mesh simplification will also be explored. The retaining of anatomical information with finer detail will be provided a higher cost while reconstructing meshes for visualization, as opposed to regions which could be handled with lower mesh sizes. Due to the exploratory nature of the project, the use of the device was only tested with a mannequin. The next step is to use the setup in a cadaver lab at the University of Washington. This will be extended for use during live surgery for studying the benefits of HoloLens in the operating theater.

In addition to using gestures for controlling holograms, voice commands will be incorporated to provide surgeons a secondary method of communication with the HoloLens. Voice commands can be used to start the holographic rendering process, for scaling objects, manipulating data or for object placement. The robust voice recognition system employed on the HoloLens device consists of multiple microphones which can perform well despite the background noise from equipment present in operating rooms.

A user interface will be developed to provide a simple interaction module that surgeons can seamlessly navigate and use throughout the surgery. This will be mindfully developed by surveying and including UI factors that would provide a steady transition for surgeons to view, dissect and study the volumetric data. A software for preoperative planning of skull base surgery is under development at the BioRobotics Lab. The models generated will be introduced onto the HoloLens device to enable surgeons to collaboratively visualize surgical plans and use this information to increase the quality of tumor

margin excision through augmented reality. The use of the HoloLens device can also be extended for object tracking to provide information about the distance between instrument tip and tissue in real-time. The large deformations that occur due to breathing need to be accounted for during registration.

ACKNOWLEDGMENT

REFERENCES

[1] J. C. Hu, X. Gu, and S. R. Lipsitz, Comparative effectiveness of minimally invasive vs open radical prostatectomy, Journal of American Medical Association, vol. 302, no. 14, pp. 15571564, 2009.

[2] K. Nagpal, K. Ahmed, A. Vats, D. Yakoub, D. James, H. Ashrafian, A. Darzi, K. Moorthy, and T. Athanasiou, Is minimally invasive surgery beneficial in the management of esophageal cancer? A meta-analysis, Surgical Endoscopy, vol. 24, no. 7, pp. 16211629, 2010.

[3] D. W. Easter, A surgeons perspective on laparoscopic cholecystectomy, AJR Am. J. Roentgenol., vol. 157, no. 2, pp. 241242, Aug. 1991.

[4] U. Sure, O. Alberti, M. Petermeyer, R. Becker, and H. Bertalanffy, Advanced image-guided skull base surgery, Surg. Neurol., vol. 53, no. 6, pp. 563572, Jun. 2000.

[5] S. DiMaio, T. Kapur, K. Cleary, S. Aylward, P. Kazanzides, K. Vosburgh, R. Ellis, J. Duncan, K. Farahani, H. Lemke, T. Peters, WB. Lorensen, D. Gobbi, J. Haller, LL Clarke, S. Pizer, R. Taylor, R. Galloway Jr, G. Fichtinger, N. Hata, K. Lawson, C. Tempany, R. Kikinis, and F. Jolesz, Challenges in Image-Guided Therapy System Design, NeuroImage, vol. 37, no. 0 1, pp. S144 S151, 2007.

[6] P. Breedveld, H. G. Stassen, D. W. Meijer, and L. P. S. Stassen, Theoretical background and conceptual solution for depth perception and eye-hand coordination problems in laparoscopic surgery, Minim. Invasive Ther. Allied Technol., vol. 8, no. 4, pp. 227234, 1999.

[7] K. Ikeda, S. Saitoh, A. Tsubota, Y. Arase, K. Chayama, H. Kumada, G. Watanabe, and M. Tsurumaru, Risk factors for tumor recurrence and prognosis after curative resection of hepatocellular carcinoma, Cancer, vol. 71, no. 1, pp. 1925, Jan. 1993.

[8] A. B. Adegbite, M. I. Khan, K. W. E. Paine, and L. K. Tan, The recurrence of intracranial meningiomas after surgical treatment, J. Neurosurg., vol. 58, no. 1, pp. 51 56, Jan. 1983.

[9] L.-M. Su, B. P. Vagvolgyi, R. Agarwal, C. E. Reiley, R. H. Taylor, and G. D. Hager, Augmented Reality During Robot-assisted Laparoscopic Partial Nephrectomy: Toward Real-Time 3D-CT to Stereoscopic Video Registration, Urology, vol. 73, no. 4, pp. 896900, Apr. 2009

[10] Y. Sato, M. Nakamoto, Y. Tamaki, T. Sasama, I. Sakita, Y. Nakajima, M. Monden, and S. Tamura , Image guidance of breast cancer surgery using 3-D ultrasound images and augmented reality visualization, IEEE Trans. Med. Imaging, vol. 17, no. 5, pp. 681693, 1998.

[11] H. Liao, T. Inomata, I. Sakuma, and T. Dohi, Threedimensional augmented reality for mriguided surgery using integral videography auto stereoscopic-image overlay, IEEE Trans. Biomed. Eng., vol. 57, no. 6, pp. 14761486, 2010.

[12] H. Fuchs, M. A. Livingston, R. Raskar, A. Colucci, K. Keller, A. State, J. R. Crawford, P. Rademacher, S. H. Drake, and A. A. Meyer, Augmented reality visualization for laparoscopic surgery, in International Conference on Medical Image Computing and Computer-Assisted Intervention, 1998, pp. 934943.

[13] A. Elmi-Terander, H. Kulason, M. Sderman, J. Racadio, R. Homan, D. Babic, N. van der Vaart, and R. Nachabe, Surgical Navigation Technology Based on Augmented Reality and Integrated 3D Intraoperative Imaging: A Spine Cadaveric Feasibility and Accuracy Study, Spine, vol. 41, no. 21, pp. E1303E1311, Nov. 2016.

[14] R. Wen, C. B. Chng, C. K. Chui, K. B. Lim, S. H. Ong, and S. K. Y. Chang, Robot-assisted RF ablation with interactive planning and mixed reality guidance, in 2012 IEEE/SICE International Symposium on System Integration (SII), 2012, pp. 3136.

[15] V. Ferrari, G. Megali, E. Troia, A. Pietrabissa, and F. Mosca, A 3-D Mixed-Reality System for Stereoscopic Visualization of Medical Dataset, IEEE Trans. Biomed. Eng., vol. 56, no. 11, pp. 26272633, Nov. 2009.

[16] W. E. Lorensen and H. E. Cline, Marching Cubes: A High Resolution 3D Surface Construction Algorithm, in Proceedings of the 14th Annual Conference on Computer Graphics and Interactive Techniques, New York, NY, USA, 1987, pp. 163169.

[17] Asset Store. [Online]. Available: https://www.assetstore.unity3d.com/en/#!/content/43658. [Accessed: 06-Jun-2017].

[18] J. R. Shewchuk, Delaunay refinement algorithms for triangular mesh generation, Comput. Geom., vol. 22, no. 13, pp. 2174, 2002.

[19] N. Kalavakonda, "Isosurface Visualization Using Augmented Reality for Improving Tumor Resection Outcomes", University of Washington, 2017.

[20] Stphane Nicolau, Xavier Pennec, Luc Soler, and Nicholas Ayache. 2003. "Evaluation of a new 3D/2D registration criterion for liver radiofrequencies guided by augmented reality." In Proceedings of the 2003 international conference on Surgery simulation and soft tissue modeling (IS4TM'03). Springer-Verlag, Berlin, Heidelberg, 270-283.